

Scalar and vector probabilistic seismic hazard analysis: application for Algiers City

Gherboudj Faouzi · Laouami Nasser

Received: 5 February 2013 / Accepted: 24 June 2013 / Published online: 20 July 2013
© Springer Science+Business Media Dordrecht 2013

Abstract This study deals with the application of probabilistic seismic hazard analysis (PSHA) for a rock site located in Algiers city. For this purpose, recent ground motion prediction equations developed in the world for similar sismotectonic context are used through logic tree in PSHA framework; the obtained results reflect clearly the high seismicity of the considered region. Moreover, deaggregation analysis is conducted to obtain the mean scenario in terms of magnitude and distance. In addition to the scalar-PSHA, a new method named vector-PSHA developed in recent years is performed in this study. Based on the multivariate probability theory, the software used in scalar approach is modified allowing the application of this approach for a real site in Algiers city with a vector of two and three parameters of intensity measure. The results are presented in terms of the joint annual rate of exceeding several thresholds such as PGA , $PSA(T)$ of multiple vibration periods, peak ground velocity and Arias intensity and comparison between results of PSHA and V-PSHA is done.

Keywords PSHA · Vector-PSHA · Intensity measure · Deaggregation · Algiers

1 Introduction

The principal objective of seismic hazard analysis is to estimate the likelihood that different levels of intensity measures will be experienced at a site. In Algeria, Many studies of seismic hazard have been carried using both deterministic and probabilistic approach and the results were often presented in terms of hazard curves (Bouhaded and Laouami 2002) and hazard maps (Pelaez et al. 2003, 2005) and the seismic loads are defined in the Algerian seismic code (RPA) based on the hazard maps of peak ground acceleration (PGA) for different return periods. In this study, based on previous studies of sismotectonic and seismic hazard of Algeria (Meghraoui 1988, Meghraoui 1992a, b; Boudiaf 1996; Geomatrix and CGS 1998; Hamdache 1998; Harbi et al. 2007; Maouche et al. 2011) probabilistic seismic hazard analysis (PSHA) for a rock site located in Algiers city is conducted with considering several intensity measures like PGA , pseudo spectral acceleration (PSA)(T), peak ground velocity (PGV), and Arias intensity (A_i). The seismic model incorporates geologic, geodetic, and instrumental seismology data and considers the background earthquakes as point sources located at depth between 0 and 20 Km, which conforms to the observed depth of almost all events that has occurred in the region.

Recently, a new method has been presented by Bazzurro (1998) named Vector-PSHA which expresses

G. Faouzi (✉) · L. Nasser
National Earthquake Engineering Research Center (CGS),
Rue Kaddour Rahim,
BP. 252, Hussein Dey, Algiers, Algeria
e-mail: gherboudj_faouzi@yahoo.fr

G. Faouzi
Faculty of Civil Engineering, University of Science
and Technology Houari Boumediene (USTHB),
BP 32 El Alia, Bab Ezzouar,
Algiers 16111, Algeria

the joint annual rate of exceedance of two or more intensity measures; it allows improving therefore the characterization of the future ground motion. Furthermore, Bazzurro et al. (2009) introduced an indirect method in which one doesn't need modification of the PSHA's software by just using some manipulation of PSHA results such as the hazard curves of different intensity measures and conditional distributions of magnitude and distance from deaggregation. However, this method has almost not been used in seismic hazard studies, maybe because of its computational demanding effort.

In the present work, PSHA's software is modified to perform vector-PSHA (V-PSHA), the means and the standard deviations of the multivariate normal distribution of two and three intensity measures are computed based on the multivariate probability theory. The annual joint rate of exceedance of two and three intensity measures such as *PGA*, *PSA*, *PGV* and A_i are computed and compared with results from PSHA.

2 Scalar probabilistic seismic hazard analysis

2.1 PSHA background

Conventional scalar-PSHA allows the computation of the annual mean rate at which a particular intensity measure *IM* (e.g., *PGA*, *PGV*, *PSA(T)*) will adopt a certain value.

Equation (1) gives the mathematical description of PSHA, it integrates over all possible ground motion scenarios defined in terms of magnitude (*M*), distance (*R*) and other seismological parameters (θ) from the *N* sources located in the surrounding area as follows:

$$\lambda_{IM}(im) = \sum_{i=1}^{N_{sources}} \lambda_i \left\{ \iint P(IM > im) f_{M,R}(m, r) dm dr \right\}_i \tag{1}$$

Where:

λ_i is the activity rate of the earthquake greater than M_{min} for source *i*.

$f_{M,R}(m, r)$ is the joint probability density function of magnitude *M*, distance *R* for source *i*.

and:

$$P(IM > im) = 1 - \Phi(\varepsilon_{im}) \tag{2}$$

$$\varepsilon_{im} = \frac{(\ln im - \mu_{\ln IM|m,r})}{\sigma_{\ln IM|m,r}} \tag{3}$$

Where Φ is the standard Gaussian CDF, and ε_{im} named the epsilon is number of standard deviation by which the logarithmic of the threshold level of any ground motion parameters deviate from the median value predicted by a ground motion prediction equation (*GMPE*) given *M*, *R* and θ .

The variation of ground motion in terms of magnitude, distance and θ is expressed using ground motion prediction models *GMPEs* which has the general form as follow:

$$\ln(IM) = \widehat{\ln IM}(M, R, \theta) + \sigma(M, R, \theta) \cdot \varepsilon_{im} \tag{4}$$

And therefore, the variability of the empirical intensity parameters $\ln(IM)$ around the median value $\widehat{\ln IM}(M, R, \theta)$ for the same seismological parameters (*M*, *R* and θ) is accounted by the standard deviation σ .

2.2 Site-specific scalar-PSHA computation

2.2.1 Description of the site

A real rock site located in Algiers city is considered in this study at the coordinate of 3.05 E; 36.75 N. This region has suffered frequently from destructive moderate to strong earthquakes. The considered site is located very close to Sahel fault, south Metodija basin fault, and Zemourri fault. The last one was responsible for the 2003 Boumerdes earthquake (M_w 6.8), the earthquake characteristic model is considered. The characteristic earthquake recurrence rate was calculated using the seismic moment estimated from the presumed geological slip rate and fault geometry as suggested by Youngs and Coppersmith (1985).

The seismicity parameters for the north Algeria source areas such as *a* and *b* values for Gutenberg–Richter relationship and the maximum expected magnitudes M_{max} were computed by Hamdache (1998) and Hamdache et al. (1998). The maximum magnitude was calculated using the statistical procedure of Kijko and Sellevoll (1989).

2.2.2 Hazard curves

Algiers falls within an area of active shallow crustal seismicity, and therefore, the *GMPEs* of Akkar and Bommer (2010), Boore and Atkinson (2008), Ambraseys et al. (2005) and Berge-Thierry et al. (2003) are employed to compute the ground motion

intensity (*PGA*, *PSA* (*T*)) at the considered site. An equal weight is assigned to each equation within the logic tree framework.

Hazard curve is the basic result of PSHA, it shows the probability of exceeding a ground motion level for a range of ground motion values. Figure 1 shows the hazard curves for short and long periods (*PGA*, *PSA* (*T*=0.2 s) and *PSA* (*T*=0.5 s), *PSA* (*T*=1 s) and *PSA* (*T*=2 s)). These curves reflect the high seismicity of the Algiers area and reveal that for the commonly used return period of 475 years, the expected mean ground motion values for different periods are *PGA*=4.3 m/s², *PSA*(0.2 s)=10.28 m/s², *PSA*(0.5 s)=6.0 m/s², *PSA*(1.0 s)=3.14 m/s², and *PSA*(2.0 s)=1.2 m/s². It is important to underline that these obtained accelerations are more important than those proposed by the Algerian seismic code.

In this study, we extend the analysis to other ground motion parameters such as *PGV* and *Ai*. The equations of Akkar and Bommer (2010) and the equation of Danciu and Tselentis (2007) are used for *PGV* and *Ai*, respectively, and the results in Figs. 2 and 3 show relatively high values such as *PGV*=20.48 cm/s and *Ai*=80.46 cm/s for the 475 years return period.

2.2.3 Deaggregation

Deaggregation analysis for the considered site is conducted and the mean scenarios in terms of *magnitude and distance* associated with a corresponding 475 years return period or 10 % 50 year probability of exceedance are computed. Figures 4 and 5, respectively, present the deaggregation results for *PSA* at 0.2 and 1 s.

At short periods such as 0.2 s, the seismic hazard at Algiers city is dominated by mean scenarios $M_{\text{mean}}=6.3$ at close source-to-site distance $R_{\text{mean}}=16$ km, and at intermediate periods, such as 1.0 s, the seismic hazard is governed by strong earthquake $M_{\text{mean}}=6.8$ at a larger distance $R_{\text{mean}}=26$ km.

3 Vector probabilistic seismic hazard analysis

3.1 V-PSHA formulation

V-PSHA has the same concept of PSHA; it expresses the annual joint rate of event with two or more of intensity measures exceeding specific threshold levels. It has been developed in recent years with the assumption of the

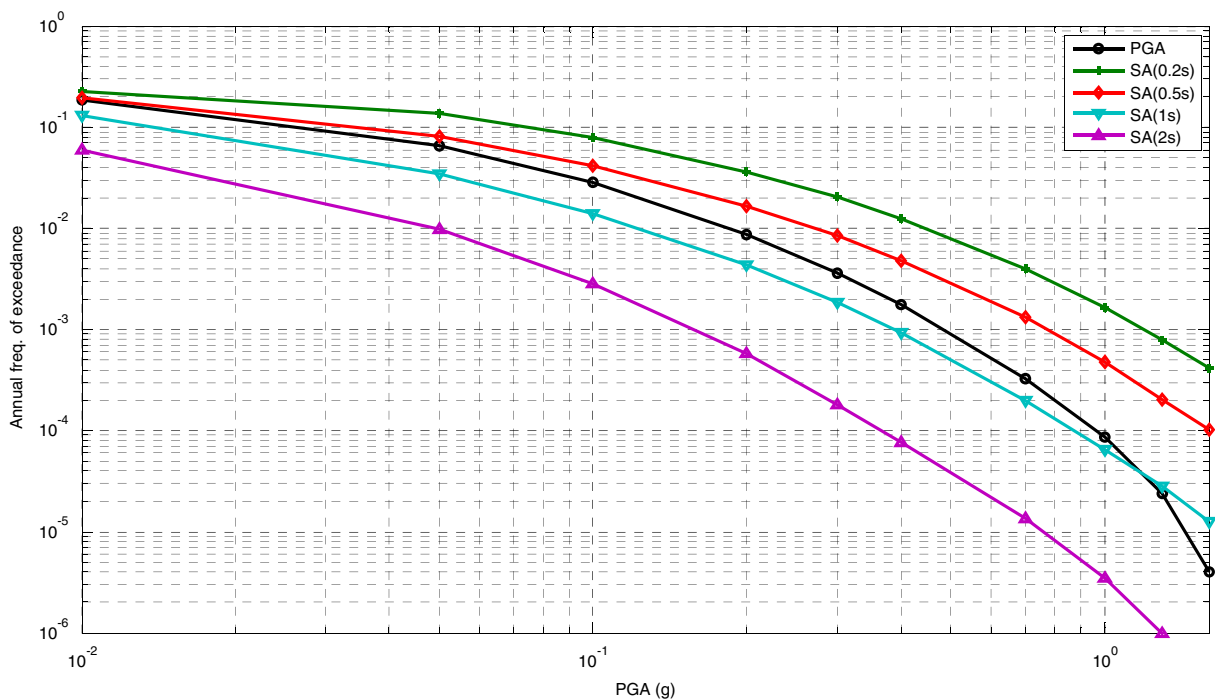


Fig. 1 Mean hazard curves at the considered site for *PGA*, pseudo spectral acceleration (*PSA*) (*T*=0.2 s), *SA* (*T*=0.5 s), *SA* (*T*=1 s) and *SA* (*T*=2 s)

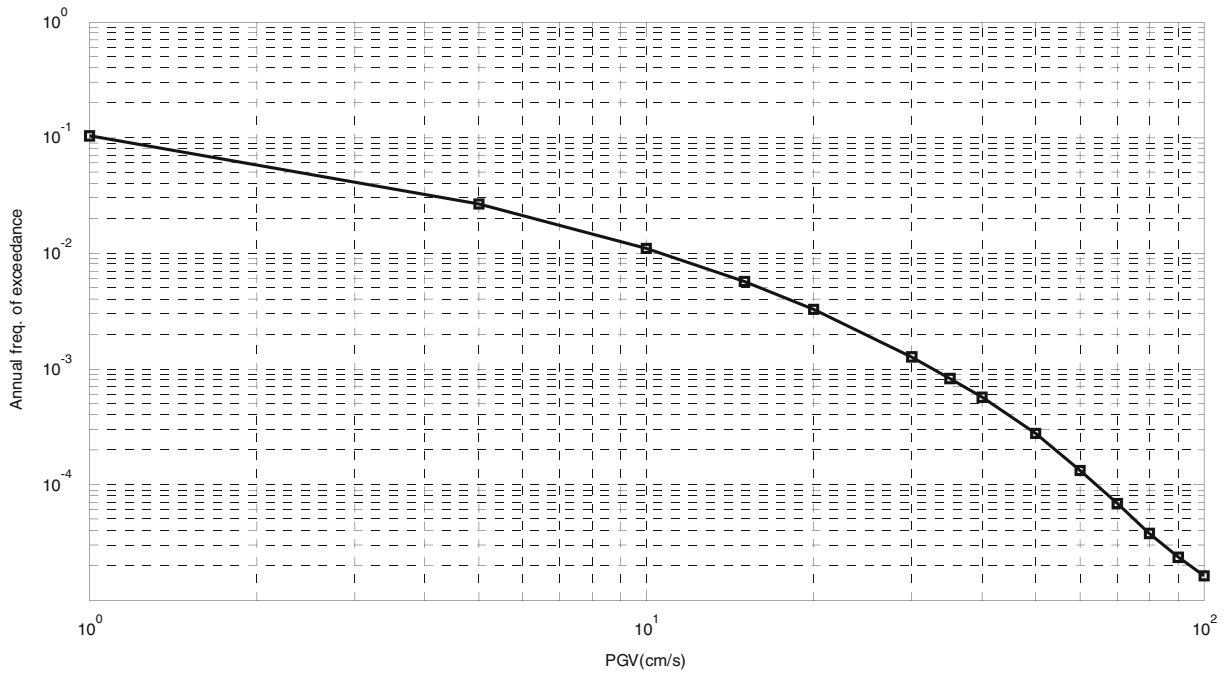


Fig. 2 Mean hazard curves at the considered site for PGV

multivariate lognormal distribution for all considered intensity measures.

Equation 5 gives an example of the formulation of 3D V-PSHA with three ground motion intensity

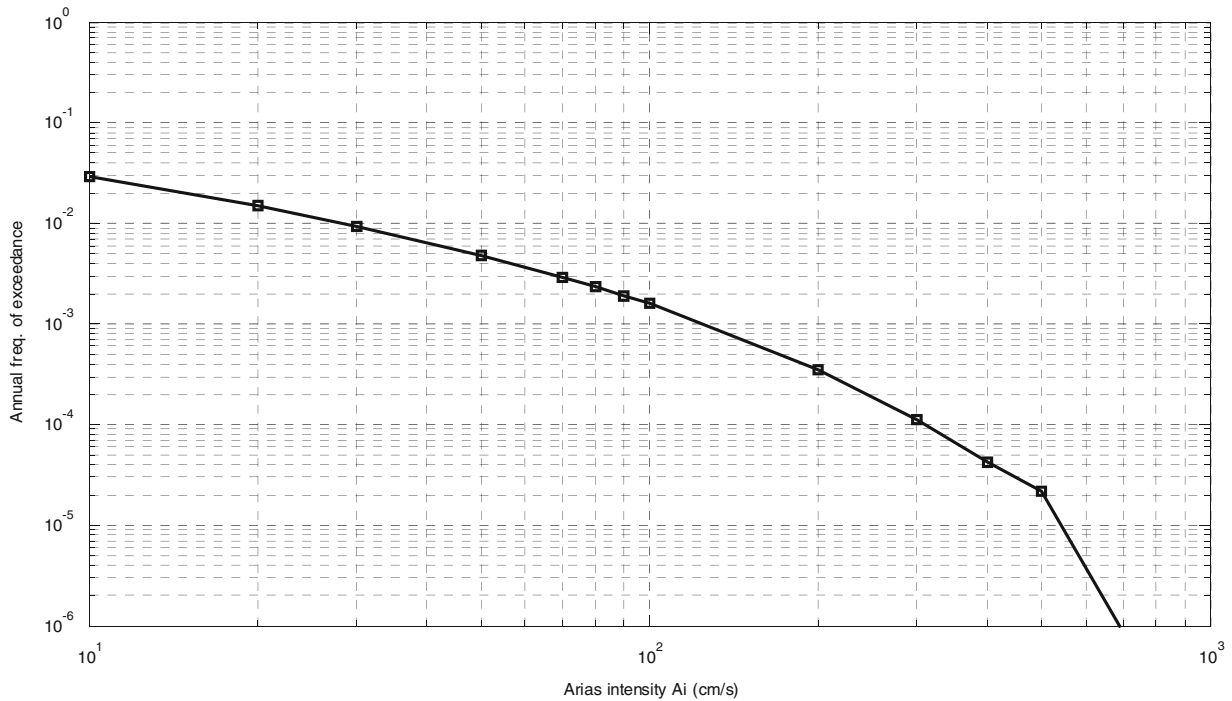


Fig. 3 Mean hazard curves at the considered site for Arias intensity A_i

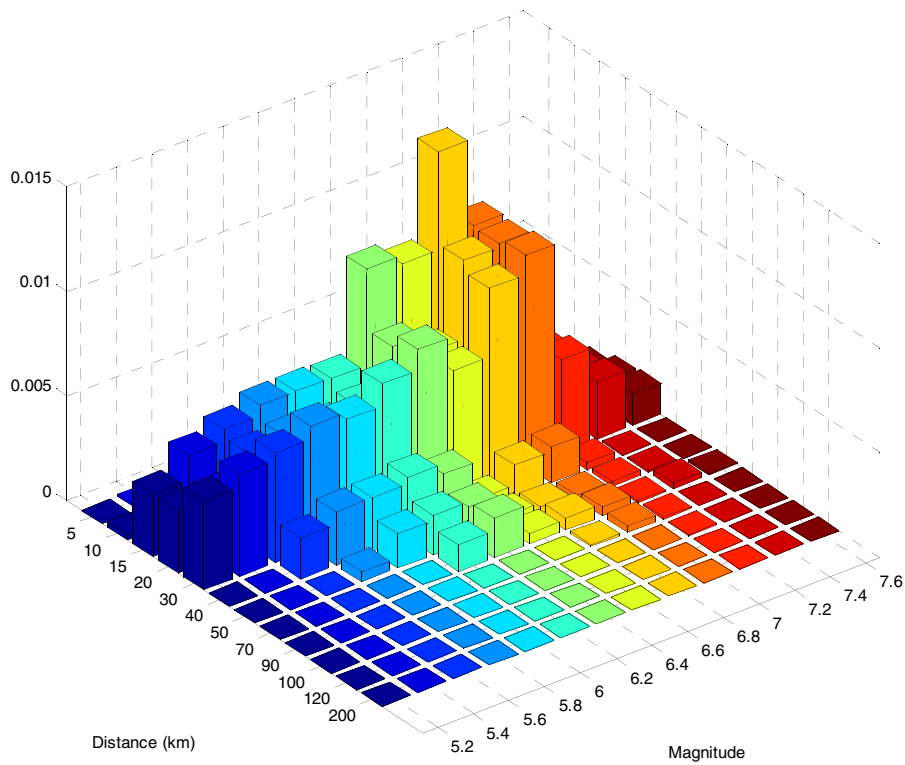


Fig. 4 Disaggregation at the considered site for $PSA(0.2\text{ s})$ at 475-year return period $\lambda(PSA(T=0.2\text{ s}))=0.0021$, $M_{\text{mean}}=6.3$, $R_{\text{mean}}=16\text{ Km}$

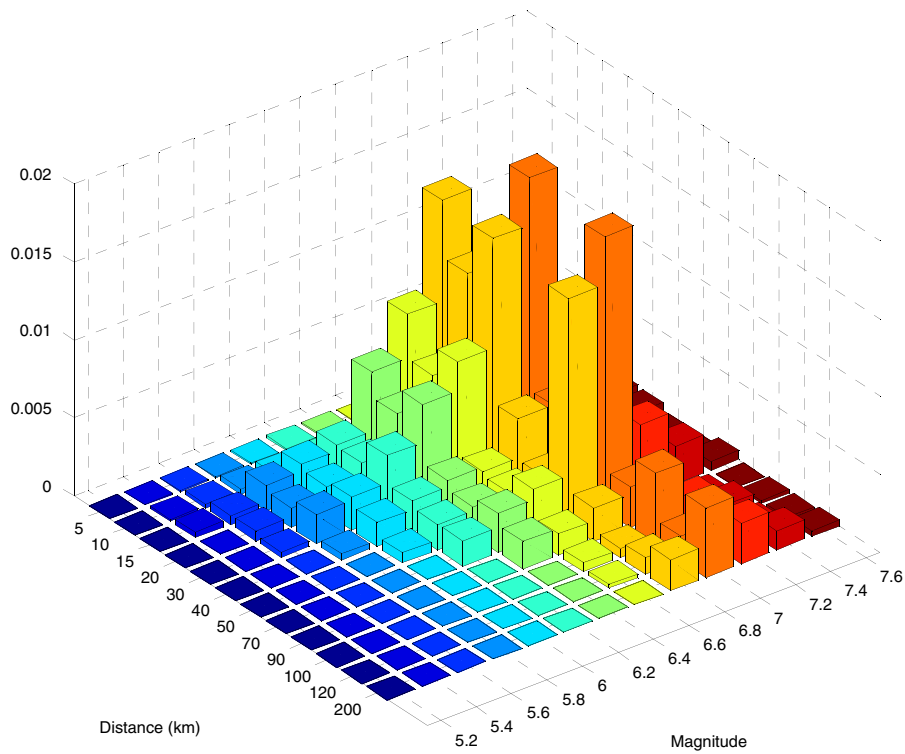


Fig. 5 Disaggregation at the considered site for $PSA(1\text{ s})$ at 475-year return period $\lambda(PSA(T=1\text{ s}))=0.0021$, $M_{\text{mean}}=6.8$, $R_{\text{mean}}=26\text{ Km}$

measures IM_1 , IM_2 and IM_3 . The mean annual rate of exceeding the threshold levels im_1 , im_2 and

im_3 , respectively, is described mathematically as follow:

$$\lambda_{IM_1,IM_2,IM_3}(im_1, im_2, im_3) = \sum_{i=1}^N \lambda_i \left\{ \iiint P(IM_1 > im_1, IM_2 > im_2, IM_3 > im_3 | m, r) f_{M,R}(m, r) dm dr \right\}_i \quad (5)$$

Where:

λ_i is the activity rate for source i

and the probability of exceeding i can be computed as follow:

$$P(IM_1 > im_1, IM_2 > im_2, IM_3 > im_3 | m_i, r_i) = \iiint_{im_1, im_2, im_3}^{\infty} f(IM_1, IM_2, IM_3 | m_i, r_i) dim_1 dim_2 dim_3 \quad (6)$$

The joint probability density function $f(IM_1, IM_2, IM_3 | m_i, r_i)$ in Eq. 6 can be rewritten in the conditional form:

$$f(IM_1, IM_2, IM_3 | m_i, r_i) = f(IM_1 | IM_2, IM_3, m_i, r_i) f(IM_2 | IM_3, m_i, r_i) f(IM_3 | m_i, r_i) \quad (7)$$

Based on the assumption of multivariate normal distribution between ground motion intensity measure IM_i , the mean and standard deviation of the distribution $f(IM_1 | IM_2, IM_3, m_i, r_i)$ are computed using the variance–

covariance matrix (Σ) defined as:

$$\Sigma = \begin{pmatrix} \sigma_1^2 & \rho_{12}\sigma_1\sigma_2 & \rho_{13}\sigma_1\sigma_3 \\ \rho_{12}\sigma_1\sigma_2 & \sigma_2^2 & \rho_{23}\sigma_2\sigma_3 \\ \rho_{13}\sigma_1\sigma_3 & \rho_{23}\sigma_2\sigma_3 & \sigma_3^2 \end{pmatrix} \quad (8)$$

σ_1 , σ_2 and σ_3 are the values of standard deviation derived from ground motions prediction models of the corresponding ground motion parameters IM_1 , IM_2 and IM_3 , respectively, that correspond to each couple of magnitude distance m_i, r_i .

ρ_{12} , ρ_{13} and ρ_{23} are correlation coefficients between each pair of these parameters.

The mean and standard values of the first parameter conditioned on the two other parameters ($\mu(IM_1 | IM_2, IM_3, m_i, r_i)$, $\sigma(IM_1 | IM_2, IM_3, m_i, r_i)$) for each couple m_i, r_i are then computed following the multivariate probability theory as follow:

$$\mu(IM_1 | IM_2, IM_3, m_i, r_i) = \left\{ \mu_{\ln M_1} + [\rho_{12}\sigma_1\sigma_2 \quad \rho_{13}\sigma_1\sigma_3] \begin{bmatrix} \sigma_2^2 & \rho_{23}\sigma_2\sigma_3 \\ \rho_{23}\sigma_2\sigma_3 & \sigma_3^2 \end{bmatrix}^{-1} \begin{bmatrix} \ln im_2 - \mu_{\ln IM_2} \\ \ln im_3 - \mu_{\ln IM_3} \end{bmatrix} \right\}_{m_i, r_i} \quad (9)$$

$$\sigma^2_{(IM_1 | IM_2, IM_3, m_i, r_i)} = \left\{ \sigma_1^2 - [\rho_{12}\sigma_1\sigma_2 \quad \rho_{13}\sigma_1\sigma_3] \begin{bmatrix} \sigma_2^2 & \rho_{23}\sigma_2\sigma_3 \\ \rho_{23}\sigma_2\sigma_3 & \sigma_3^2 \end{bmatrix}^{-1} \begin{bmatrix} \rho_{12}\sigma_1\sigma_2 \\ \rho_{13}\sigma_1\sigma_3 \end{bmatrix} \right\}_{m_i, r_i} \quad (10)$$

The distribution $f(IM_2 | IM_3, m_i, r_i)$ is easier to define by the mean and the median values calculated for each couple (m_i, r_i) as follow:

$$\mu(IM_2 | IM_3, m_i, r_i) = \left\{ \mu_{\ln M_2} + \frac{\rho_{23}\sigma_2}{\sigma_3} * (\ln im_3 - \mu_{\ln IM_3}) \right\}_{m_i, r_i} \quad (11)$$

$$\sigma_{(IM_2 | IM_3, m_i, r_i)} = \left\{ \sigma_{\ln IM_2} + \sigma_{\ln IM_2} \sqrt{1 - \rho_{23}^2} \right\}_{m_i, r_i} \quad (12)$$

Several correlation models have been developed for different intensity measures that allow computing the

Table 1 Correlation models selected for each pair of intensity measures considered

	PGA	PSA at various periods	PGV	Arias intensity
PGA	Unity	Baker and Jayaram (2008)	Bradley (2012)	Baker (2007)
PSA at various periods	Symmetric	Baker and Jayaram (2008)	Bradley (2012)	Baker (2007)
PGV	Symmetric	Symmetric	Unity	Aochi and Douglas (2006)
Arias intensity	Symmetric	Symmetric	Symmetric	Unity

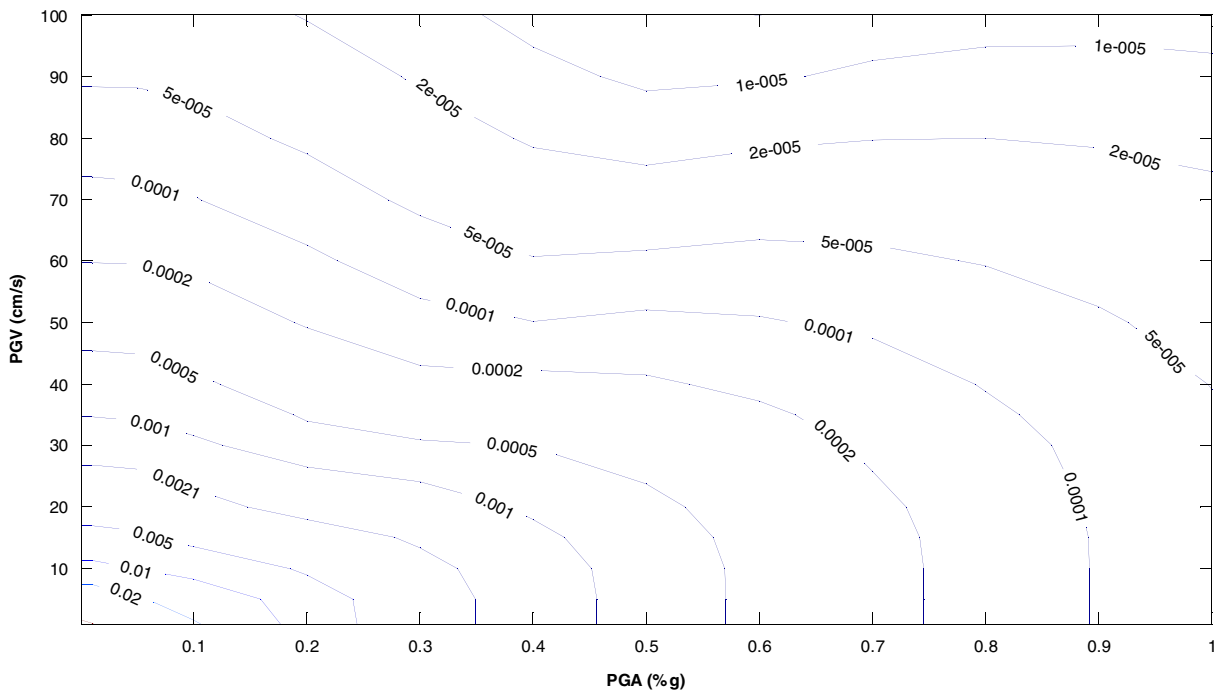


Fig. 6 Seismic hazard contours (mean annual joint rates of exceedance) for the pair of (PGA, PGV)

correlations coefficients (ρ_{ij}), Baker (2007) presents correlation models between Arias intensity and PSA

for a range of structural periods. Moreover, Baker and Jayaram (2008) provide models of the correlations

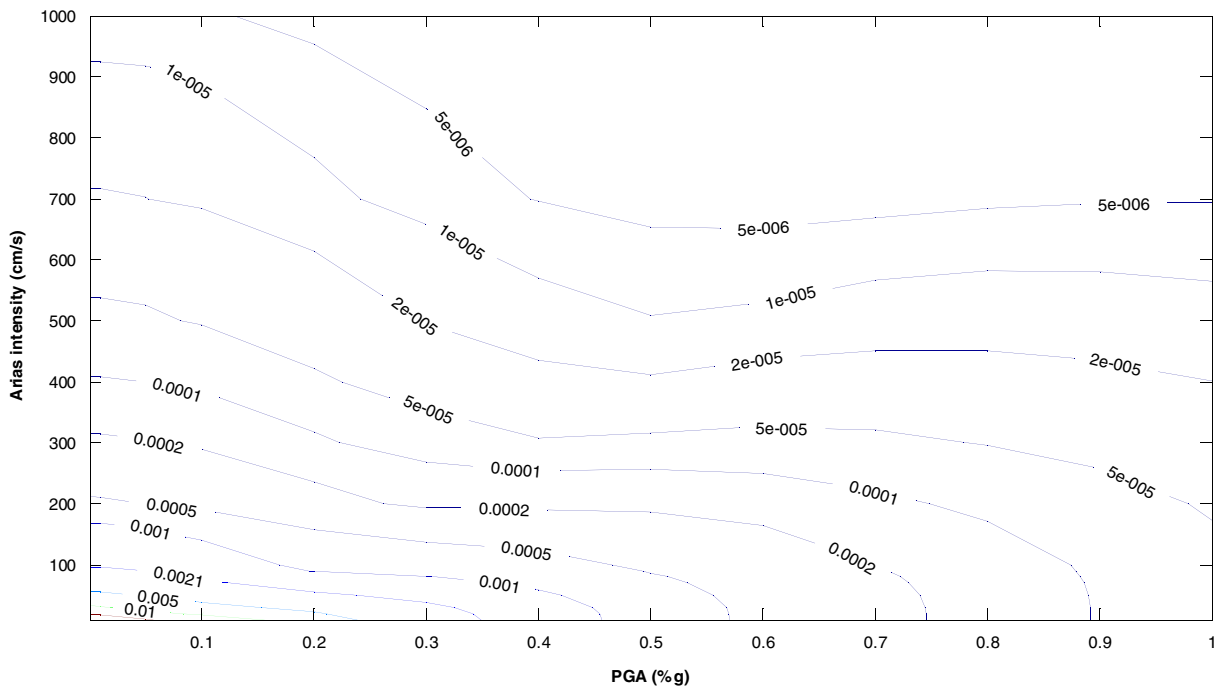


Fig. 7 Seismic hazard contours (mean annual joint rates of exceedance) for the pair of (PGA, A_i)

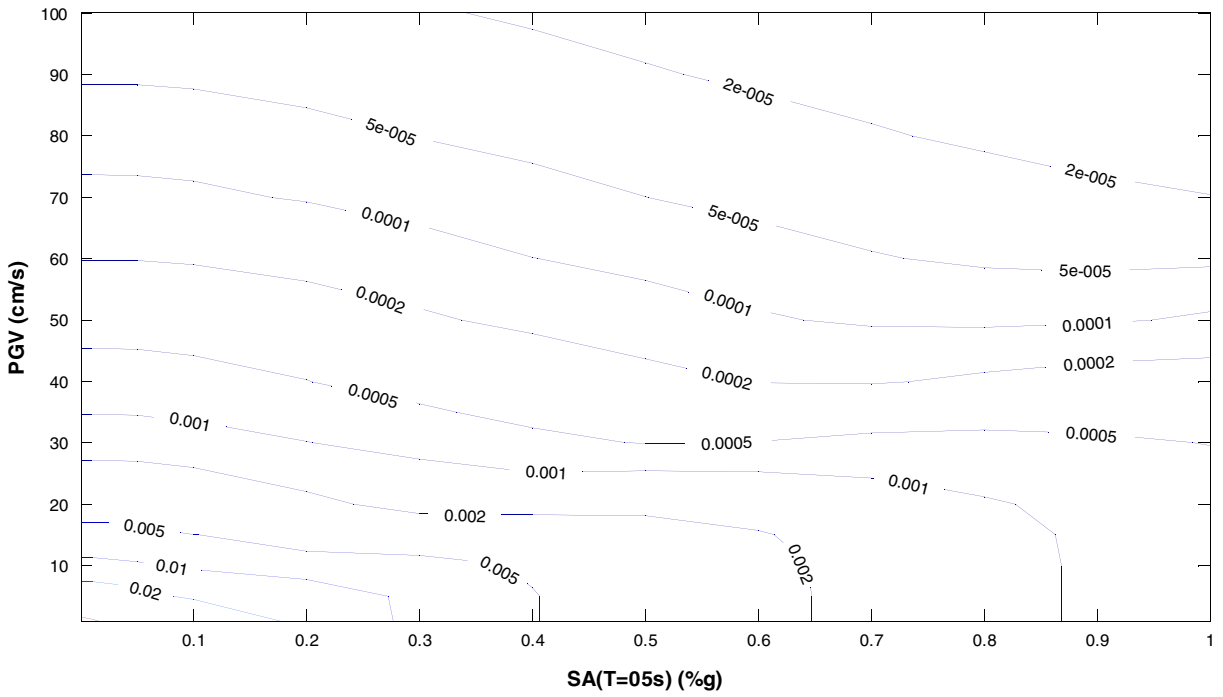


Fig. 8 Seismic hazard contours (mean annual joint rates of exceedance) for the pair of $(PSA(0.5\text{ s}), PGV)$

between $PSAs$ for different structural periods based on analysis of a large dataset and for recent

GMPEs. Bradley (2011) studied the correlations between relative significant duration and various

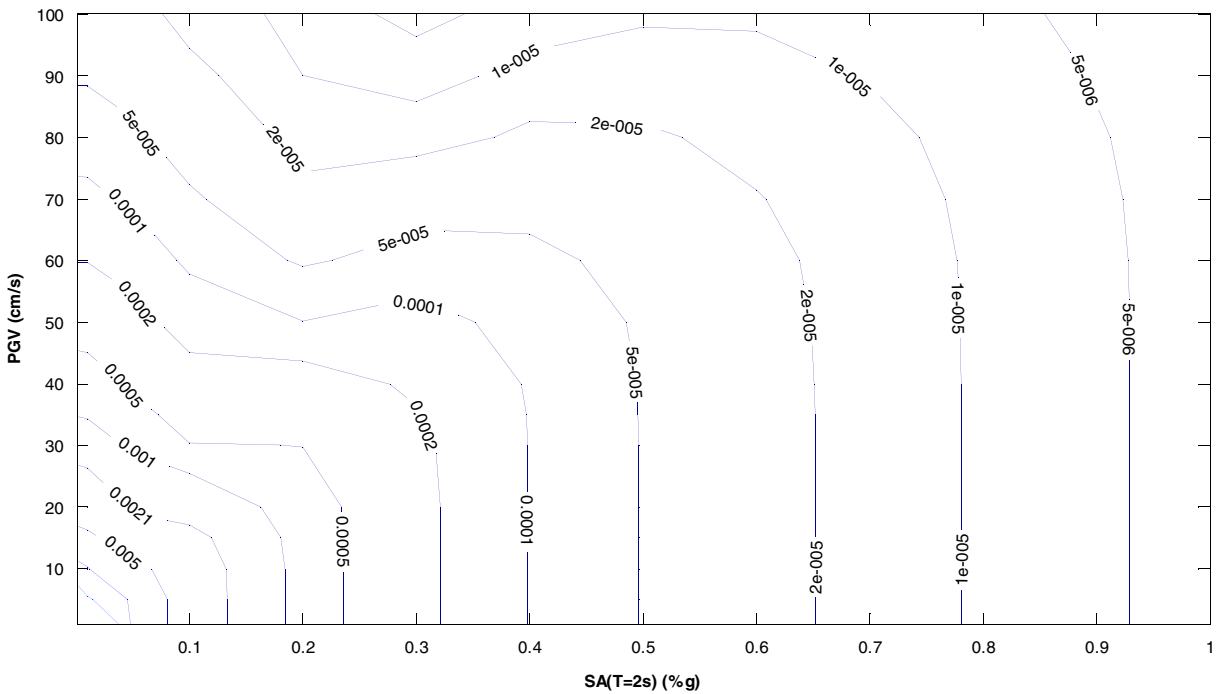


Fig. 9 Seismic hazard contours (mean annual joint rates of exceedance) for the pair of $(PSA(2\text{ s}), PGV)$

other intensity measures like *PGA*, *PGV*, *A_i* and *PSA*.

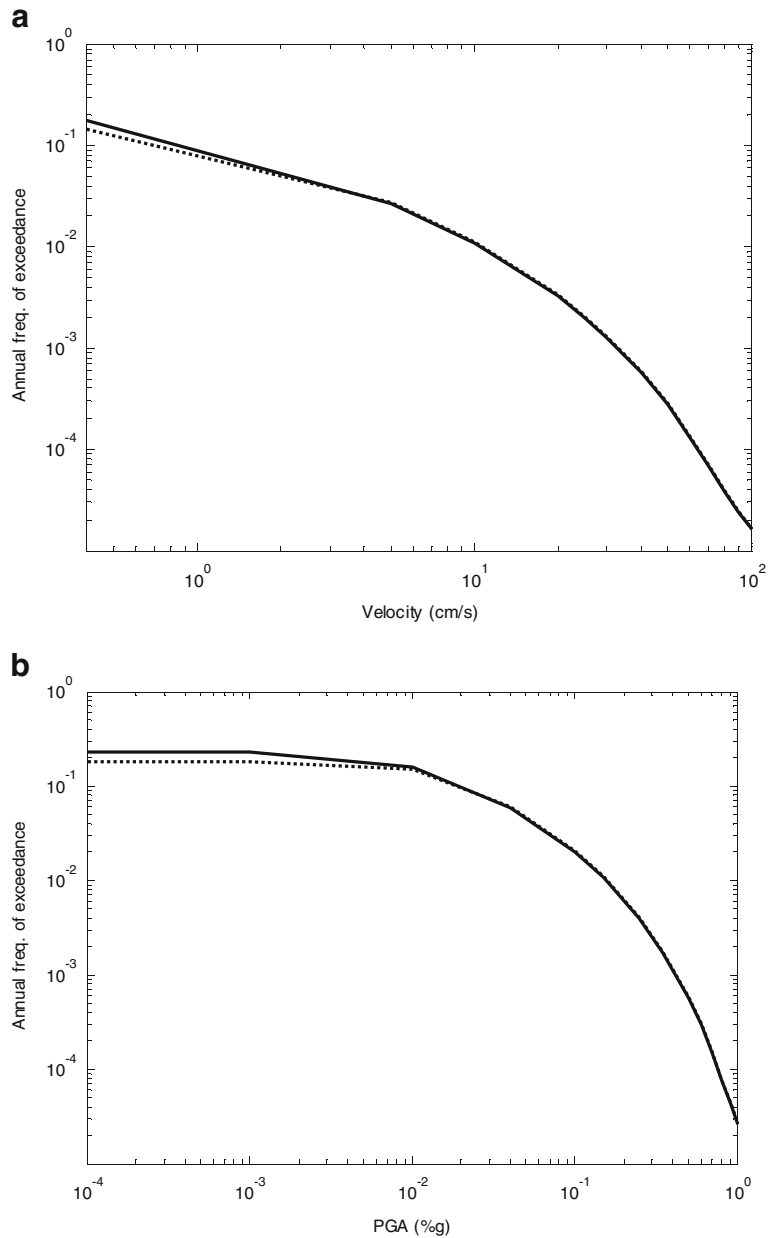
3.2 Site-specific V-PSHA application

The application of V-PSHA becomes possible with the availability of several correlations models between different intensity measures. Table 1 summarises the correlation models selected for each pair of intensity measures considered in this study.

2D V-PSHA is applied by using Eqs. (11–12). Figures (6, 7, 8 and 9) show the computed mean rates of exceedance for four pairs of the considered intensity measures at the Algiers site (*PGA-PGV*, *PSA (T=0.5)-PGV*, *PSA (T=0.5)-A_i* and *PSA (T=2)-A_i*).

The marginal distributions along the *x*- and *y*-axes of the contour plots shown in Figs. (6, 7 and 8) should correspond to the scalar-valued PSHA hazard curves shown in Figs. (1, 2 and 3). Since along the axes, the probabilities correspond to one of the *IMs* being greater

Fig. 10 Comparison between PSHA and 2D V-PSHA results for *PGA* and *PGV*



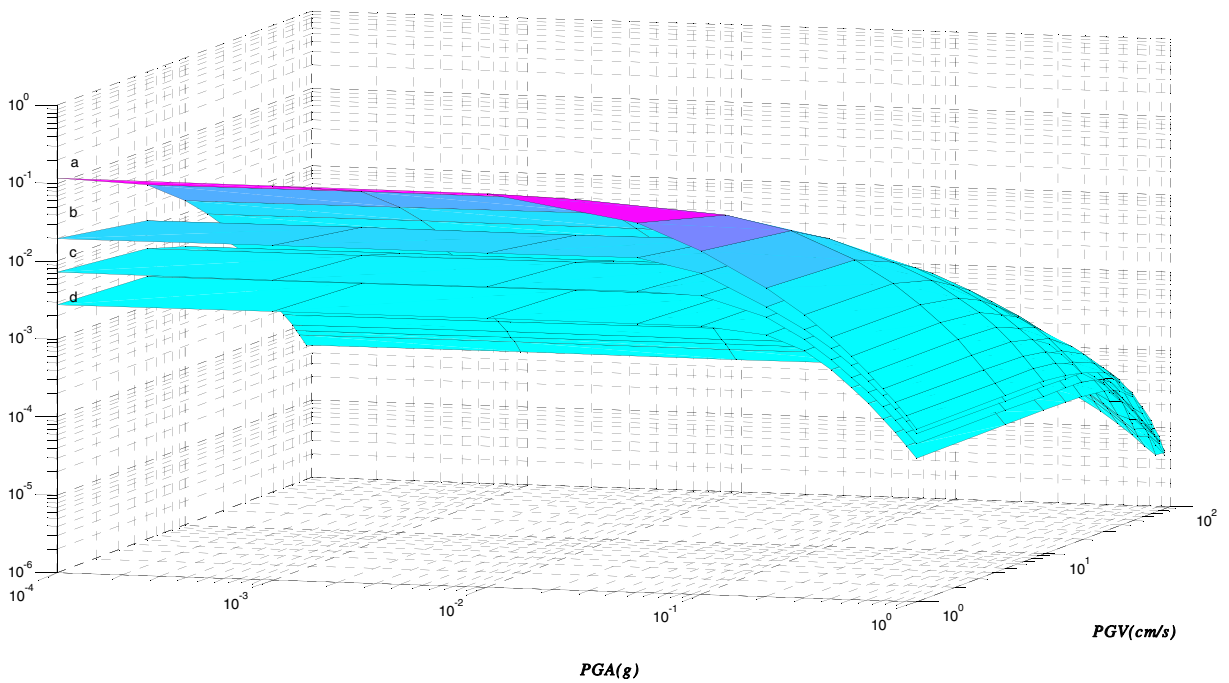


Fig. 11 MAR of exceeding a triples of *PGA*, *PGV* and Arias intensity at the Casbah site during the same earthquake. *a* MRE ($PGA \geq x, PGV \geq y, A_i \geq 1 \text{ cm/s}$) *b* MRE ($PGA \geq x, PGV$

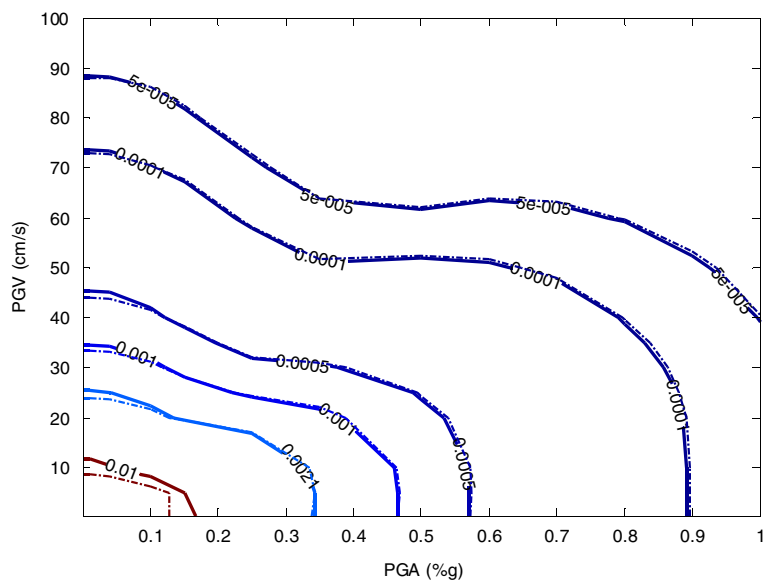
$\geq y, A_i \geq 20 \text{ cm/s}$) *c* MRE ($PGA \geq x, PGV \geq y, A_i \geq 50 \text{ cm/s}$), *d* MRE ($PGA \geq x, PGV \geq y, A_i \geq 100 \text{ cm/s}$)

than zero (the *x*-axis corresponds to the probability that $PGA > 0$ and the *y*-axis corresponds to the probability that $PGV > 0$), this characteristic provides a way of checking that modified software is being performed correctly. Figure 10a, b compares the marginal distributions from the contour plots to the standard hazard

curves for *PGA* and *PGV*. It shows that for this pair of *IMs*, the marginal distributions quite closely match those scalar-valued hazard curves.

Following Eq. 5–10, 3D V-PSHA is conducted. Figure 11 shows the results in terms four surface plots of the joint mean annual rates of exceeding three

Fig. 12 Comparison between 2D and 3D V-PSHA with ($A_i > 0 \text{ cm/s}$)



threshold levels corresponding to three intensity measures PGA , PGV and A_i . Each surface plots the joint hazard for PGA , PGV and A_i ($PGA \geq x$, $PGV \geq y$, $A_i \geq z$ cm/s) corresponds to one value of z (1, 20, 50, 100 cm/s).

For checking the results of 3D V-PSHA, we compare the hazard contours of the PGA - PGV pair obtained by 2D V-PSHA shown in Fig. 6 with hazard contours of 3D V-PSHA in terms of PGA , PGV and A_i corresponding to $A_i > 0$. It is shown in Fig. 12 that the contours obtained from 3D V-PSHA based on multivariate probability theory closely match the contours obtained from a direct integration method of 2D V-PSHA.

4 Conclusion

In this study, scalar and vector probabilistic seismic hazard analysis methods are described and conducted for a rock site located in Algiers city; for this purpose, several intensity measures are considered such as PGA , $PSA(T)$, PGV and Arias intensity A_i . Those parameters could have great importance in the risk assessment of buildings and geotechnical structures. In general terms, the obtained results reflect clearly the high seismicity of the considered region. We also show that the seismic hazard for PGA and PSA of both short and intermediate period is dominated by events of medium to high magnitude, usually ($M_w > 6.0$) for 475 years return period.

Based on the theoretical assumption of multivariate distribution of intensity measures, V-PSHA is performed in this study by modifying the classical software of PSHA; results are presented in terms of the annual joint mean rate of exceeding of two and three value's thresholds of different intensity measures. These results allow the characterization of several aspects of strong ground motion thought probabilistic seismic hazard analysis which could improve the prediction of damage in structural and geotechnical engineering problems.

References

- Akkar S, Bommer JJ (2010) Empirical equations for the prediction of PGA , PGV , and spectral accelerations in Europe, the Mediterranean Region and the Middle East. *Seismol Res Lett* 81:195–206
- Ambraseys NN, Douglas J, Sarma SK (2005) Equations for the estimation of strong ground motions from shallow crustal earthquakes using data from Europe and the Middle East: horizontal peak ground acceleration and spectral acceleration. *Bull Earthq Eng* 3(1):1–53. doi:10.1007/s10518-005-0183-0
- Aochi H, Douglas J (2006) Testing the validity of simulated strong ground motion from the dynamic rupture of a finite fault, by using empirical equations. *Bull Earthq Eng* 4(3):211–229. doi:10.1007/s10518-006-0001-3
- Baker JW (2007) In: Takada, Furuta (eds) Correlation of ground motion intensity parameters used for predicting structural and geotechnical response. Applications of statistics and probability in civil engineering—Kanda. Taylor & Francis Group, London, ISBN 978-0-415-45134-5
- Baker JW, Jayaram N (2008) Correlation of spectral acceleration values from NGA ground motion models. *Earthquake Spectra* 24(1):299–317
- Bazzurro P (1998) Probabilistic seismic demand analysis, Ph. D. Dissertation, Dept. of Civil and Environmental Engineering, Stanford University, Stanford, CA
- Bazzurro P, Tothong P, Park J (2009) Efficient Approach to Vector-valued Probabilistic Seismic Hazard Analysis of Multiple Correlated Ground motion Parameters, ICOSAR 2009, Safety, Reliability and Risk of Structures, Infrastructures and Engineering Systems, Furuta, Frangopol & Shinozuka, London
- Berge-Thierry F, Cotton C, Scotti O, Griot-Pommer DA, Fukushima Y (2003) New empirical response spectral attenuation laws moderate European earthquakes. *J Earthq Eng* 7(2):193–222
- Boore DM, Atkinson GM (2008) Ground-motion prediction equations for the average horizontal component of PGA , PGV , and 5%-damped PSA at spectral periods between 0.01 s and 10.0 s. *Earthquake Spectra* 24(1):99–138
- Boudiaf A (1996) Etude sismotectonique de la région d'Alger et de la Kabylie (Algérie). PhD thesis, University of Montpellier, p 274
- Bouhaded Y, Laouami N (2002) Earthquake hazard assessment in the Oran region (Northwest Algeria). *Nat Hazard* 26:227–243
- Bradley BA (2011) Correlation of significant duration with amplitude and cumulative intensity measures and its use in ground motion selection. *J Earthq Eng* 15(6):809–832
- Bradley BA (2012) Empirical correlation peak ground velocity and spectrum-based intensity measures. *J Earthquake Spectra* 28(1):17–35
- Danciu L, Tselentis GA (2007) Engineering ground-motion parameters attenuation relationships for Greece. *Bull Seismol Soc Am* 97(1B):162–183. doi:10.1785/0120040087
- Geomatrix Consultants, Inc, and National center of earthquake engineering research (CGS) (1998) Probabilistic hazard assessment of the the Algiers region. UNCH project No. ALG/92/003, Technical Rapport submitted to United Nation Centre for Human Settlements, Nairobi, Kenya, 53 pp., plus Tables, figures and plates. doi:10.1029/2004GL021646
- Hamdache M (1998) Seismic hazard assessment for the main seismogenic zones in north Algeria. *Pure Appl Geophys* 152:281–314
- Hamdache M, Bezzeghoud M, Mokrane A (1998) Estimation of seismic hazard parameters in the northern part of Algeria. *Pure Appl Geophys* 151:101–117
- Harbi A, Maouche S, Vaccari F, Aoudia A, Oussadou F, Panza GF, Benouar D (2007) Seismicity, seismic input and site effects in the Sahel—Algiers region (North Algeria). *Soil Dyn Earthq Eng* 27:427–447

- Kijko A, Sellevol MA (1989) Estimation of earthquake hazard parameters from incomplete data files Part I. Utilization of extreme and complete catalog with different threshold magnitudes *bull. Seismol Soc Am* 79(3):645–654
- Maouche S, Meghraoui M, Morhange C, Belabbes S, Bouhadad Y, Haddoum H (2011) Active coastal thrusting and folding, and uplift rate of the Sahel Anticline and Zemmouri earthquake area (Tell Atlas, Algeria). *Tectonophysics*. doi:10.1016/j.tecto.2011.06.003
- Meghraoui M (1988) Géologie des zones sismiques du Nord de l'Algérie. PhD Thesis, Université de Paris-Sud Centre d'Orsay, pp 355
- Meghraoui M (1992a) Active folds and their seismotectonic implication of the Tellian Mountains of Algeria. *Quaternary Research Association, Cambridge*, p 36
- Meghraoui M (1992b) Paleoseismicity of active thrust faults—the El Asnam (Algeria) case study. *Neotectonics—recent advances: abstract volume*. Quaternary Research Association, Cambridge, p 37
- Pelaez JA, Hamdache M, Lopez Casado C (2003) Seismic hazard in northern Algeria using spatially smoothed seismicity. *Tectonophysics* 372:105–119
- Pelaez JA, Hamdache M, Lopez Casado C (2005) Updating the probabilistic seismic hazard values of northern Algeria with the 21 May 2003 M 6.8 Algiers earthquake included. *Pure Appl Geophys* 162:2163–2177
- Youngs RR, Coppersmith K (1985) Implications of fault slip rates and earthquake recurrence models to probabilistic seismic hazard estimates. *Bull Seismol Soc Am* 58:939–964